Biochemical and Biophysical Research Communications 427 (2012) 207–211

Contents lists available at SciVerse ScienceDirect

Biochemical and Biophysical Research Communications

journal homepage: www.elsevier.com/locate/ybbrc

Identification of structural traits that increase the antimicrobial activity of a chimeric peptide of human β-defensins 2 and 3

Björn Spudy [a], Frank D. Sönnichsen [b], Georg H. Waetzig [c], Joachim Grötzinger [a,*], Sascha Jung [a]

[a] Institute of Biochemistry, Christian-Albrechts-University, Olshausenstr. 40, 24098 Kiel, Germany
[b] Otto Diels Institute of Organic Chemistry, Christian-Albrechts-University, Olshausenstr. 40, 24098 Kiel, Germany
[c] CONARIS Research Institute AG, Schauenburgerstr. 116, 24118 Kiel, Germany

ARTICLE INFO

Article history:
Received 31 August 2012
Available online 18 September 2012

Keywords:
Human beta-defensin
Structure
Antimicrobial peptide
Antimicrobial activity
NMR

ABSTRACT

Antimicrobial peptides participate in the first line of defence of many organisms against pathogens. In humans, the family of β-defensins plays a pivotal role in innate immunity. Two human β-defensins, β-defensin-2 and -3 (HBD2 and HBD3), show substantial sequence identity and structural similarity. However, HBD3 kills *Staphylococcus (S.) aureus* with a 4- to 8-fold higher efficiency compared to HBD2, whereas their activities against *Escherichia (E.) coli* are very similar. The generation of six HBD2/HBD3-chimeric molecules led to the identification of distinct molecular regions which mediate their divergent killing properties. One of the chimeras (chimera C3) killed both *E. coli* and *S. aureus* with an even higher efficacy compared to the wild-type molecules. Due to the broad spectrum of its antimicrobial activity against many human multidrug-resistant pathogens, this HBD2/HBD3-chimeric peptide represents a promising candidate for a new class of antibiotics. In order to investigate the structural basis of its exceptional antimicrobial activity, the peptide's tertiary structure was determined by NMR spectroscopy, which allowed its direct comparison to the published structures of HBD2 and HBD3 and the identification of the activity-increasing molecular features.

1. Introduction

The first (passive) line of defence of an organism against pathogens is the physical barrier of the epidermis. The second (active) line of defence is constituted by epithelial cells, which are able to produce and secrete antimicrobial peptides (AMPs), and thereby prevent the infiltration of pathogens into the organism [1]. The innate immune system of invertebrates and vertebrates is armoured with a large group of antimicrobial peptides, often also called host defence peptides [2–5]. One important group of AMPs consists of the defensins, which contain six cysteine residues arranged in three intramolecular disulphide bonds [5]. Due to the localization and pairing of these six cysteine residues, the defensins are classified into three subgroups, namely the α-, β-, and θ-defensins [5].

The human β-defensins HBD2 and HBD3 were primarily isolated from keratinocytes of patients with psoriasis [6,7]. Apart from the skin, they are also present in heart and skeletal muscle, placenta, epithelia of the trachea and lung tissues [8]. Both peptides are inducible by bacterial challenge and proinflammatory cytokines such as tumour necrosis factor-α (TNF-α,) interferon-γ (IFN-γ) and interleukin-1β (IL-1β) [6,9–11].

HBD2 and HBD3 share a characteristic fold composed of three-stranded anti-parallel β-sheets and a short N-terminal α-helix [12,13]. The tertiary structures of both peptides have been determined, but their mechanism of bacterial cell membrane permeabilisation is still not known in detail. Structural studies have shown that both HBD2 and HBD3 can form dimers in solutions, albeit at high concentrations in the case of HBD2 [12,13]. Dimers of HBD2 were proposed to form an octamer, which does not seem to generate membrane-spanning pores but rather disrupts the bacterial cell membrane by electrostatic interactions [12]. Furthermore, HBD3 was shown to generate ion channels in oocytes of *Xenopus laevis* [14]. Although both peptides show substantial sequence identity and structural similarity, they clearly differ in their antimicrobial activity with respect to the target pathogens. HBD3 kills *Staphylococcus aureus* with a 4- to 8-fold higher efficiency compared to HBD2, whereas their activities against *Escherichia coli* are very similar [15].

Recently, we generated six chimeric HBD2/HBD3 molecules (C1–C6) and studied their antimicrobial activity against *E. coli* and *S. aureus* strains [15]. The chimera C3 showed a drastically enhanced activity compared to its parent molecules and even killed a broad panel of multidrug-resistant pathogens [15]. In order to investigate the structural basis of its improved function in

* Corresponding author. Address: Biochemisches Institut, Christian-Albrechts-Universität zu Kiel, Olshausenstrasse 40, 24118 Kiel, Germany. Fax: +49 431 8805007.
E-mail address: jgroetzinger@biochem.uni-kiel.de (J. Grötzinger).

0006-291X/$ - see front matter © 2012 Elsevier Inc. All rights reserved.
http://dx.doi.org/10.1016/j.bbrc.2012.09.052

comparison to the parent peptides, the chimera's tertiary structure was determined by NMR spectroscopy in the present study. It facilitated the identification of the activity-increasing molecular traits of C3 by comparison with the wild-type peptides HBD2 and HBD3. These results provide the basis for a complete understanding of the mechanism of action of human β-defensins and for the improvement of designer HBD2/HBD3 chimeras.

2. Materials and methods

2.1. Peptide synthesis

The chimera C3 was chemically synthesized by Biosyntan (Berlin, Germany) using standard Fmoc-based solid-phase synthesis according to the method of Jung et al. [15]. The lyophilised peptide was reconstituted in 10 mM HCl with a final peptide concentration of 1 mg/ml. This stock solution was diluted 1:40 in refolding buffer (50 mM Tris–HCl, 1 M guanidine hydrochloride, 4 mM reduced glutathione, 0.4 mM oxidised glutathione, pH 8.5) and incubated at 37 °C overnight. After incubation, the buffer was exchanged to 50 mM sodium phosphate (pH 6.0) by dialysis. The renaturated C3 was purified by reverse-phase high-performance liquid chromatography (RP-HPLC) using C18 columns (Macherey–Nagel, Düren, Germany) and acetonitrile–trifluoroacetic acid in the mobile phase. The fraction containing C3 was freeze-dried.

2.2. Circular dichroism spectroscopy

Circular dichroism (CD) measurements were performed on a Jasco J-720 spectropolarimeter (Japan Spectroscopic, Tokyo, Japan) using quartz cuvettes with specific path lengths (Hellma, Müllheim, Germany). The spectropolarimeter was calibrated according to the method of Chen and Yang [16]. Each CD spectrum represents the mean of three scans at a bandwidth of 2 nm and a data pitch of 1 nm. The scanning speed was adjusted to 5 nm/min with a response time of 8 s. Heat stability of C3, which was dissolved in 20 mM sodium phosphate (pH 4.6), was determined by recording the CD signal at 230 nm and by changing the temperature from 20 to 90 °C and vice versa. All other CD spectra were recorded at 20 °C.

CD experiments were also performed in the absence or presence of liposomes in order to compare the secondary structure of C3 in aqueous and hydrophobic environments. Liposomes were prepared essentially as described by Pick et al. [17] using defined phospholipids and 50 mM sodium phosphate buffer (pH 5.2). Initially, crude liposome samples were refined by passing them over a NAP-5 column (GE Healthcare, Freiburg, Germany). The eluate served as a stock suspension for the subsequent experiments and was stored at 4 °C. L-α-phosphatidyl-DL-glycerol (PG) phospholipids were purchased from Avanti Polar Lipids (Alabaster, AL). Due to the net negative charge at the membrane surface, PG liposomes serve as highly simplified models for bacterial membranes. Liposome suspension diluted 1:100 in 50 mM sodium phosphate buffer (pH 7.0) was applied to one chamber of a tandem quartz cuvette (2 × 4.375 mm) to a final volume of 800 µl. The other chamber was filled with the same volume of peptide sample (16 µg/ml) dissolved in the same buffer as the liposomes. After initial measurement of separated peptide and liposome samples, the tandem cuvette was inverted 40× to mix the samples. Spectra of the mixed samples were recorded after 20 min of incubation.

2.3. Sample preparation and NMR experiments

Freeze-dried C3 was dissolved in 20 mM sodium phosphate (pH 4.6) in 93% (v/v) H_2O and 7% (v/v) D_2O. For determination of hydrogen bonds by hydrogen–deuterium exchange, freeze-dried C3 was dissolved in 20 mM sodium phosphate (pH 4.6) in 100% (v/v) D_2O. NMR measurements were performed on a Bruker Avance 600-MHz spectrometer equipped with a z-gradient triple resonance cryoprobe using matched microtubes (Shigemi, Allison Park, PA). Sequence-specific backbone resonance assignments of the peptide were established using the following spectra: two-dimensional total correlation spectroscopy (TOCSY) with mixing times of 60, 85, and 120 ms, respectively, and nuclear Overhauser effect spectroscopy (NOESY) with mixing times of 60, 80, 100, 120, 150 and 200 ms, respectively. All spectra were acquired at 298 K, processed with the software NMRPipe [18], referenced to the water resonance at 4.75 ppm, and analysed with the software NMRView [19]. The chemical shift data were deposited in the University of Wisconsin Biological Magnetic Resonance Bank database under accession number 18684.

2.4. Structure calculations

Structure calculations were performed using the software CYANA [20]. The calculations were based on 517 interproton constraints derived from the NOESY experiment with a 120 ms mixing time. Distances were calibrated so that the median NOE intensity corresponded to a distance of 2.7 Å with a tolerance of 0.125 × the bound-squared. Methyl intensities were divided by 2.0. All lower bounds were set to 1.8 Å. Furthermore, three disulphide bonds were defined as nine distance restraints ranges as follows: $2.0 \le d(S_i^{\gamma},\ S_j^{\gamma}) \le 2.1$ Å; $3.0 \le d(C_i^{\beta},\ S_j^{\gamma}) \le 3.1$ Å; $3.0 \le d(S_i^{\gamma},\ C_j^{\beta}) \le 3.1$ Å. In addition, 12 distance restraints ranges from 6 hydrogen bonds were set to 1.8–2.0 Å between the donor hydrogen atom and the acceptor oxygen atom and 2.7–3.0 Å between the donor nitrogen atom and the acceptor oxygen atom. Two hundred structures were calculated, of which twenty structures with the lowest target functions were selected as the final structural ensemble and were deposited (Protein Data Bank code 2lxo). The average structure was calculated from the ensemble of these 20 structures using the software WHAT IF [21] and subsequently energy minimised using the GROMOS force field [22].

2.5. Graphic representations

All molecular graphical representations were generated using the software MOLMOL [23] and GRASP2 [24].

3. Results

3.1. CD spectroscopy

The shape of the CD spectra of C3 is characteristic for peptides containing β-sheets (Fig. 1). The thermal stability was examined by increasing the temperature stepwise and recording the CD signal at 230 nm. As shown in Fig. 1, the CD signal decreased slightly but continuously with increasing temperature. We observed no distinct transition point, which would indicate denaturation. Furthermore, CD-spectra at 20 °C, recorded before and after heating, exhibited the same shape (Fig. 1). Therefore, C3 possesses high temperature stability. In the presence of model membranes (PG liposomes) mimicking bacterial cell membranes with a net negative surface charge, C3 undergoes a conformational change. The maximum at 230 nm, which is typical for β-sheet peptides, was drastically changed (Fig. 1). Due to the interaction with membranes, C3 exhibited a CD spectrum characteristic for peptides of partial α-helix content with minima around 222 nm and 208 nm.

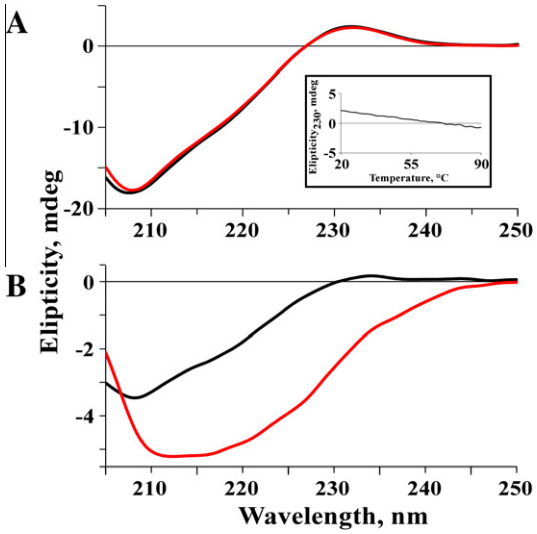

Fig. 1. Heat stability of chimera C3 and its interaction with model membranes. The ellipticity is depicted as a function of wavelength from 205 to 250 nm. (A), CD spectra from heat stability measurements both recorded at 20 °C. Black, CD spectrum of C3 before heating to 90 °C. Red, CD spectrum of C3 after heating to 90 °C and cooling down. Inset, ellipticity measured at 230 nm while increasing temperature from 20 to 90 °C. (B), CD spectra of C3 in the absence (black) or presence (red) of PG liposomes serving as model membranes.

3.2. Tertiary structure of chimera C3

The structural statistics for the calculation of the structure of C3 are summarised in Table 1.

Like its parental peptides HBD2 and HBD3, C3 folds into a cysteine-stabilized α/β fold and adopts an overall similar conformation. C3 contains an N-terminal α-helix followed by a double-stranded β-sheet (Fig. 2A). The chimera's N-terminal segment, i.e., its primary structure, is identical to that of HBD3. Therefore, it is not surprising that this part of C3 resembles more HBD3 (Fig. 2B) than HBD2 (Fig. 2C). However, the structure of C3 also shows several differences to the respective regions and overall structures of HBD2 and HBD3. The α-helical region of C3 is less pronounced than those of HBD2 and HBD3. Moreover, the longitudinal axis of the helix of C3 appears to be rotated by about 90°. In contrast to HBD2 and HBD3, which both contain a three-stranded β-sheet, C3 features only a double-stranded β-sheet. The corresponding backbone region is orientated in a perpendicular manner to the β-strands of C3, whereas in HBD2 and HBD3, the three β-strands exhibit a tilt angle of approximately 30° each. However, in all three peptides, the C-terminal β-strand is the central core region of the molecule. Moreover, in all peptides the three disulphide bridges show the same spatial arrangements.

Table 1
Structural statistics of the ensemble of 20 structures of chimera C3. None of the distance restraints was violated by more than 0.5 Å in any structure. rmsd, root mean square deviation.

Distance restraints	Number
Intraresidual ($\|i-j\|=0$)	136
Sequential ($\|i-j\|=1$)	164
Medium range ($2 \le \|i-j\| \le 4$)	91
Long range ($\|i-j\| \ge 5$)	126
Disulphide bonds (included)	24
Hydrogen bonds	18
Total	559
Pairwise rmsd for all residues 1–44	
Mean global backbone rmsd to mean	1.71 ± 0.27 Å
Mean global heavy rmsd to mean	2.28 ± 0.30 Å
Pairwise rmsd for residues 6–11 and 17–42	
Mean global backbone rmsd to mean	0.62 ± 0.13 Å
Mean global heavy rmsd to mean	1.07 ± 0.12 Å

The chimera C3 also contains structurally less defined regions. These are the peptide's N- and C-terminal regions as well as the segment between the first and the second cysteine residue (Fig. 2A and D). Interestingly, these regions are located on the same side of the molecule, whereas the opposite side is structurally much more closely defined. A fourth less defined region is localised within the small loop connecting the two β-strands.

The most prominent novel structural feature of C3 is its reduced anionic charge compared to its parental peptides (Fig. 3). The surface of C3 exhibits a large uncharged area, which is comparable to HBD2 (Fig. 3A–C, left column). However, the peptide's opposite surface possesses mainly cationic charges, a feature which is less pronounced in both HBD2 and HBD3 (Fig. 3A–C, right column). Similar to HBD3, the chimera's N-terminal region protrudes from the core of the peptide and is mainly uncharged (Fig. 3A and B). Altogether, C3 exhibits a more pronounced amphipathic character than its parental peptides.

4. Discussion

The HBD2/HBD3-chimeric peptide C3 exhibits a strongly increased antimicrobial activity and a substantially broader activity profile compared to its parental peptides [15]. Determination of the chimera's tertiary structure was performed to elucidate the structural causes for this increased activity. The solution structure of C3 showed the same characteristic overall fold of β-defensins. However, C3 clearly deviates from HBD2 and HBD3 in several regions. The most striking differences are the orientation of the α-helix and its reduced length and additionally the absence of one of the β-strands in C3. The changes in the α-helix might be a consequence of differences in the experimental conditions, which have been described to influence the length and regularity of the N-terminal helix in β-defensins. For example, α-helical content was found to be much more pronounced in X-ray structures compared to NMR structures [25]. However, the N-terminal region of C3 was identified as the functional epitope mediating the pathogen specificity of HBD3 against *S. aureus* and *E. coli* [15]. Although the contribution of the α-helix is not clear, it was described to be important for the initial interaction with bacterial membranes [26,27]. In this context, the N-terminal α-helix of HBD3 becomes stabilised when exposed to a lipid environment [28]. This is in agreement with the results from our CD-spectroscopy analyses, where a higher α-helical content of C3 was induced by the interaction with PG-liposomes mimicking bacterial membranes.

The third β-strand of HBD2 and HBD3 is replaced in C3 by a less defined loop region between the first and second cysteine residue. This structurally less defined region is a unique feature of the chimera, whereas all others are also observed in HBD2 and HBD3 [29,30]. Interestingly, HBD3 was shown to exhibit higher antimicrobial activity in its non-cysteine containing (linearised) form, which was assumed to originate in the peptide's increased flexibility [28]. However, the linearised molecule still contained some secondary structure [28,31]. Therefore, the increased antimicrobial activity of the chimera C3 appears to be a consequence of its increased flexibility in that specific region.

Another parameter correlating with the peptides' antimicrobial activity is the molecular surface electrostatic potential. Here, the charge distribution or regional charge density on the molecule's surface appears to be more important for the antimicrobial activity than the overall net charge [15,31,32]. Both HBD2 and HBD3 show clear correlations between charge and antimicrobial activity or membrane permeabilisation [12,31,32]. Interestingly, C3 exhibits a much more pronounced amphipathic character compared to its

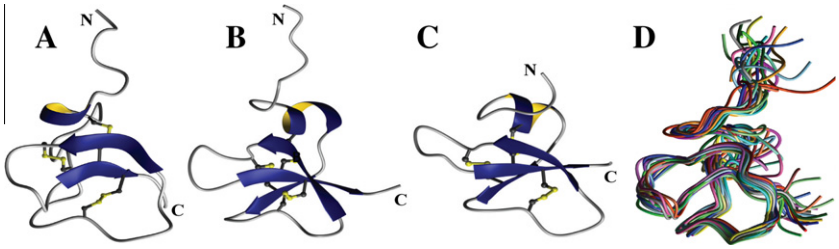

Fig. 2. Tertiary structures of chimera C3 and its parent molecules HBD2 and HBD3. The chimera's average structure (A), and the tertiary structures of HBD3 (B), and HBD2 (C), are depicted as ribbon presentations. Disulphide bonds are displayed in grey and yellow balls and sticks. Blue arrows represent β-strands, whereas the α-helices are depicted in blue and yellow. N and C denote N- and C-termini, respectively. (D), spaghetti presentation of the ensemble of 20 structures of C3 with the lowest target functions (same orientation as A).

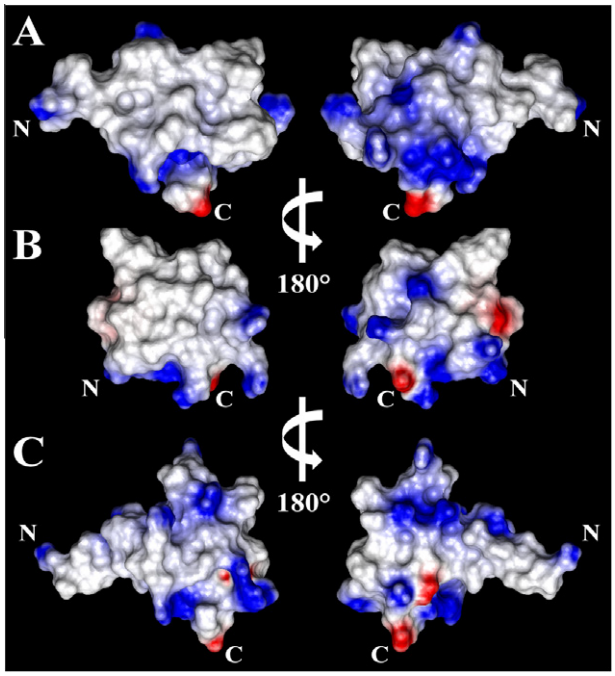

Fig. 3. Molecular surface properties of chimera C3 and its parent molecules HBD2 and HBD3. Depicted are the molecular surface electrostatic potentials of chimera C3 (A), HBD2 (B), and HBD3 (C). Blue, red and white coloured surface areas represent regions of cationic, anionic or no charge, respectively. The right column shows the molecules after 180° rotation around the vertical axis. N and C denote N- and C-termini, respectively.

parental molecules. It is has been described that the local amphipathic character of the N-termini of HBD2 and HBD3 mediates membrane insertion of the peptides [26,27]. The increased overall amphipathicity of C3 appears to support the subsequent step of membrane permeabilisation even more efficiently compared to the parental molecules.

Finally, a clear correlation exists between both the increased flexibility and amphipathicity and increased antimicrobial activity of C3. Both traits in combination appear to mediate the striking antimicrobial activity of the peptide. These results clearly show the direction for future approaches in antimicrobial peptide design. In that concern, the high temperature stability of chimera C3 is a very useful feature expanding its manageability, for example with respect to synthesis and storage.

Acknowledgments

This work was supported by the excellence cluster "Inflammation at Interfaces".

References

[1] H. Jenssen, P. Hamill, R.E. Hancock, Peptide antimicrobial agents, Clin. Microbiol. Rev. 19 (2006) 491–511.
[2] A. Izadpanah, R.L. Gallo, Antimicrobial peptides, J. Am. Acad. Dermatol. 52 (2005) 381–390 (quiz 391–382).
[3] J. Harder, R. Glaser, J.M. Schröder, Human antimicrobial proteins effectors of innate immunity, J. Endotoxin Res. 13 (2007) 317–338.
[4] M. Pazgier, D.M. Hoover, D. Yang, W. Lu, J. Lubkowski, Human beta-defensins, Cell. Mol. Life Sci. 63 (2006) 1294–1313.
[5] T. Ganz, Defensins: antimicrobial peptides of innate immunity, Nat. Rev. Immunol. 3 (2003) 710–720.
[6] J. Harder, J. Bartels, E. Christophers, J.M. Schröder, A peptide antibiotic from human skin, Nature 387 (1997) 861.
[7] J. Harder, J. Bartels, E. Christophers, J.M. Schröder, Isolation and characterization of human beta -defensin-3, a novel human inducible peptide antibiotic, J. Biol. Chem. 276 (2001) 5707–5713.
[8] R.I. Lehrer, T. Ganz, Endogenous vertebrate antibiotics. Defensins, protegrins, and other cysteine-rich antimicrobial peptides, Ann. N. Y. Acad. Sci. 797 (1996) 228–239.
[9] J. Harder, U. Meyer-Hoffert, L.M. Teran, L. Schwichtenberg, J. Bartels, S. Maune, J.M. Schröder, Mucoid *Pseudomonas aeruginosa*, TNF-alpha, and IL-1beta, but not IL-6, induce human beta-defensin-2 in respiratory epithelia, Am. J. Respir. Cell Mol. Biol. 22 (2000) 714–721.
[10] H.P. Jia, B.C. Schutte, A. Schudy, R. Linzmeier, J.M. Guthmiller, G.K. Johnson, B.F. Tack, J.P. Mitros, A. Rosenthal, T. Ganz, P.B. McCray Jr., Discovery of new human beta-defensins using a genomics-based approach, Gene 263 (2001) 211–218.
[11] J.M. Schröder, Epithelial antimicrobial peptides: innate local host response elements, Cell. Mol. Life Sci. 56 (1999) 32–46.
[12] D.M. Hoover, K.R. Rajashankar, R. Blumenthal, A. Puri, J.J. Oppenheim, O. Chertov, J. Lubkowski, The structure of human beta-defensin-2 shows evidence of higher order oligomerization, J. Biol. Chem. 275 (2000) 32911–32918.
[13] D.J. Schibli, H.N. Hunter, V. Aseyev, T.D. Starner, J.M. Wiencek, P.B. McCray Jr., B.F. Tack, H.J. Vogel, The solution structures of the human beta-defensins lead to a better understanding of the potent bactericidal activity of HBD3 against *Staphylococcus aureus*, J. Biol. Chem. 277 (2002) 8279–8289.
[14] J.R. Garcia, F. Jaumann, S. Schulz, A. Krause, J. Rodriguez-Jimenez, U. Forssmann, K. Adermann, E. Kluver, C. Vogelmeier, D. Becker, R. Hedrich, W.G. Forssmann, R. Bals, Identification of a novel, multifunctional beta-defensin (human beta-defensin 3) with specific antimicrobial activity. Its interaction with plasma membranes of Xenopus oocytes and the induction of macrophage chemoattraction, Cell Tissue Res. 306 (2001) 257–264.
[15] S. Jung, J. Mysliwy, B. Spudy, I. Lorenzen, K. Reiss, C. Gelhaus, R. Podschun, M. Leippe, J. Grötzinger, Human beta-defensin 2 and beta-defensin 3 chimeric peptides reveal the structural basis of the pathogen specificity of their parent molecules, Antimicrob. Agents Chemother. 55 (2011) 954–960.
[16] G.C. Chen, J.T. Yang, Two-point calibration of circulardichrometer with D-10-camphorsulfonic acid, Anal. Lett. 10 (1977) 1195–1207.
[17] U. Pick, Liposomes with a large trapping capacity prepared by freezing and thawing of sonicated phospholipid mixtures, Arch. Biochem. Biophys. 212 (1981) 186–194.
[18] F. Delaglio, S. Grzesiek, G.W. Vuister, G. Zhu, J. Pfeifer, A. Bax, NMRPipe: a multidimensional spectral processing system based on UNIX pipes, J. Biomol. NMR 6 (1995) 277–293.
[19] B.A. Johnson, Using NMRView to visualize and analyze the NMR spectra of macromolecules, Methods Mol. Biol. 278 (2004) 313–352.
[20] P. Güntert, Automated NMR structure calculation with CYANA, Methods Mol. Biol. 278 (2004) 353–378.
[21] G. Vriend, WHAT IF: a molecular modeling and drug design program, J. Mol. Graphics 8 (1990) 52–56 (29).
[22] W.F. van Gunsteren, S.R. Billeter, A.A. Eising, P.H. Hünenberger, P. Krüger, A.E. Mark, W.R.P. Scott, I.G. Tironi, Biomolecular Simulation: The GROMOS96 Manual and User Guide, vdf Hochschulverlag AG an der ETH Zürich, Zürich (1996) 1–1042.

[23] R. Koradi, M. Billeter, K. Wüthrich, MOLMOL: a program for display and analysis of macromolecular structures, J. Mol. Graphics 14 (1996) 51–55 (29–32).
[24] D. Petrey, B. Honig, GRASP2: visualization, surface properties, and electrostatics of macromolecular structures and sequences, Methods Enzymol. 374 (2003) 492–509.
[25] E. Klüver, K. Adermann, A. Schulz, Synthesis and structure-activity relationship of beta-defensins, multi-functional peptides of the immune system, J. Pept. Sci. 12 (2006) 243–257.
[26] M.V. Sawai, H.P. Jia, L. Liu, V. Aseyev, J.M. Wiencek, P.B. McCray Jr., T. Ganz, W.R. Kearney, B.F. Tack, The NMR structure of human beta-defensin-2 reveals a novel alpha-helical segment, Biochemistry 40 (2001) 3810–3816.
[27] K. Taylor, D.J. Clarke, B. McCullough, W. Chin, E. Seo, D. Yang, J. Oppenheim, D. Uhrin, J.R. Govan, D.J. Campopiano, D. MacMillan, P. Barran, J.R. Dorin, Analysis and separation of residues important for the chemoattractant and antimicrobial activities of beta-defensin 3, J. Biol. Chem. 283 (2008) 6631–6639.
[28] S. Liu, L. Zhou, J. Li, A. Suresh, C. Verma, Y.H. Foo, E.P. Yap, D.T. Tan, R.W. Beuerman, Linear analogues of human beta-defensin 3: concepts for design of antimicrobial peptides with reduced cytotoxicity to mammalian cells, Chem. BioChem 9 (2008) 964–973.
[29] J. Röhrl, D. Yang, J.J. Oppenheim, T. Hehlgans, Human beta-defensin 2 and 3 and their mouse orthologs induce chemotaxis through interaction with CCR2, J. Immunol. 184 (2010) 6688–6694.
[30] M.E. Selsted, A.J. Ouellette, Mammalian defensins in the antimicrobial immune response, Nat. Immunol. 6 (2005) 551–557.
[31] E. Klüver, S. Schulz-Maronde, S. Scheid, B. Meyer, W.G. Forssmann, K. Adermann, Structure-activity relation of human beta-defensin 3: influence of disulfide bonds and cysteine substitution on antimicrobial activity and cytotoxicity, Biochemistry 44 (2005) 9804–9816.
[32] Y. Bai, S. Liu, P. Jiang, L. Zhou, J. Li, C. Tang, C. Verma, Y. Mu, R.W. Beuerman, K. Pervushin, Structure-dependent charge density as a determinant of antimicrobial activity of peptide analogues of defensin, Biochemistry 48 (2009) 7229–7239.